applied sciences

MDPI

Article

Linear Tool Path-Smoothing Method in High-Speed Machining Based on Error Feasible Area and Curvature Optimization

Xuefeng Yang * and Youpeng You

College of Mechanical and Electrical Engineering, Nanjing University of Aeronautics and Astronautics, Nanjing 210016, China

* Correspondence: yangxuefeng0309@nuaa.edu.cn; Tel.: +86-13347700194

Abstract: Linear tool path is widely used in high-speed NC machining. However, the geometrical discontinuity of the corner between the linear tool paths will lead to fluctuations in speed, acceleration and jerk, which can excite machinery vibration and reduce the machining efficiency and surface quality. To solve these problems, a novel corner smoothing method based on error feasible area and curvature optimization is proposed in this paper. Compared with most traditional corner smoothing methods using higher-order curves with all control points lying in the straight segment and inside of the tool path, the proposed method constructs B-spline transition curves with smaller curvatures to smooth the corners by reasonably distributing the curve control points inside and outside the straight line segment of the tool path (i.e., error feasible area). Furthermore, the corner transition curve is optimized by the minimum curve curvature extreme to improve the smoothness of the corner transition curve and reduce fluctuation in the kinematic profiles while respecting the G^3 continuity (i.e., curvature-smooth), transition length limits and the uniqueness of curvature extremum. Finally, the simulation results show that the proposed method can reduce the curvature value and improve the smoothness of the curve and the minimum transitional velocity of the corner, which means that it can enhance machining efficiency and weaken machining vibration. The feasibility and effectiveness of the method are also verified.

Keywords: high-speed machining; error feasible area; curvature; G^3 continuity; corner smoothing

Citation: Yang, X.; You, Y. Linear Tool Path-Smoothing Method in High-Speed Machining Based on Error Feasible Area and Curvature Optimization. *Appl. Sci.* **2022**, *12*, 9443. https://doi.org/10.3390/app12199443

Academic Editor: Abílio Manuel Pinho de Jesus

Received: 31 August 2022
Accepted: 19 September 2022
Published: 21 September 2022

1. Introduction

With the development of manufacturing technology, the requirement of machining efficiency and quality is becoming more and more important in the field of molds, impellers, aerospace and other complex parts [1]. Some commercial computer-aided design (CAD)/computer-aided manufacturing (CAM) software is also widely used to generate the tool path of complex parts, which is usually represented by straight-line segments [2,3]. However, due to the discontinuity of the tangent and curvature of the corner point between the linear tool paths, the speed, acceleration and jerk are discontinuous and the phenomena of acceleration and deceleration occur frequently. These factors will reduce the machining efficiency and produce violent vibration, which will also affect the machining quality and accuracy [4]. Therefore, it is of great significance to improve the smooth transition performance of the linear tool path.

In recent years, the corner smoothing method has been an effective method for achieving a high-speed continuous motion along a linear tool path, which has been widely studied. Pessles et al. [5] and Yang KM et al. [6] inserted an arc in the middle of the double linear tool path to make the tool path reach G^1 continuity (i.e., speed-continuous). Subsequently, higher-order curves, such as Bezier, B-spline, PH or other curves were used to smooth corners and achieve G^2 continuity (i.e., curvature-continuous), which can obtain good acceleration characteristics and low machining vibration. Bi et al. [7] developed a curvature smoothing algorithm based on a cubic Bezier curve to smooth the linear tool path of

high-speed machining. This method realized G^2 continuity and improved the feed speed. A similar curve with eight control points lying in the straight segment and inside the tool path was constructed to smooth the linear tool path in Du et al. [8] and they further optimize the curvature variation energy (CVE) to obtain good motion performance. The similar distribution of control points also appears in the following literature. Pateloup et al. [9] utilized triple B-spline to connect adjacent liner tool paths and achieve G^2 continuity. The accuracy of the tool path and the smoothness of the feed speed were improved. Zhang et al. [10], Zhao et al. [11] and Han et al. [12] also used the same B-spline for realizing smaller curvature extrema to increase the transition speed. Sencer et al. [13] used quintic B-spline to smooth the path corners to ensure G^2 continuity and optimal curvature. Farouki [14] developed a corner smoothing algorithm with G^2 continuity based on the quintic PH curve. Shi et al. [15] also used the quintic PH curve to smooth the corners of a three-axis tool path, which can accurately limit the approximation error. Huang et al. [16] applied clothoid splines to develop a novel corner smoothing method with G^2 continuity.

In addition, some scholars [17–21] found that there are potentials of the G^3 (i.e., curvature-smooth) continuous tool path in suppressing machining vibration in experiments. Fan et al. [17] used two quartic Bezier curves to obtain a G^3 continuous tool path where the curvature variation energy was optimized and the G^3 tool path could generate smaller jerk than a G^2 tool path. Similarly, in our previous work, we introduced a method of generating a G^3 continuous tool path from a symmetric Bezier curve [18]. Tulsyan et al. [19] and Zhang et al. [20] applied quintic B-spline curves to obtain tool paths with G^3 continuity. An analytical NURBS curve was inserted into the corners between linear segments for improving the smoothness of the linear toolpath and the machining efficiency [21]. In addition, others also extend the smoothing methods with G^3 continuity to four-axis and five-axis tool paths [22–24]. Hu et al. [22,23] successfully developed a quintic PH spline to obtain a G^3 continuous smoothing toolpath. Sun et al. [24,25] used the Bezier curve to construct a G^3 continuous tool path in five-axis machining. This literature also verifies that a G^3 continuous path can generate smoother speed and acceleration curves, and fluctuation in the acceleration and jerk profiles is effectively constrained to obtain good machining quality.

From the above related literature, we know that a transition curve with better curvature performance can enhance machining efficiency and surface quality. When constructing the corner transition curve, the main feature of these methods is that the control points are located in the straight segment and inside between the linear tool paths and the error constraint, mainly referring the maximum error of the midpoint of a corner between linear tool paths. To obtain the smaller curvature extreme of the corner transition curve, Sun et al. [26] developed a method of connecting the linear tool path with nine control points, which lay two control points outside the straight segment of the tool path, but this method only ensured G^2 continuity. This also shows that there is still potentiality for the decrease in curvature extreme value and the improvement of smoothness at the corners. According to the above discussion, in order to ensure the surface quality and machining efficiency of the workpiece, this study reasonably determines all control points of the curve within the error feasible area of the tool path, that is, all control points can be distributed inside and outside the straight line segment of the tool path. Moreover, the curvature will be further optimized and the G^3 continuous tool path can be obtained.

The rest of this paper is arranged as follows. Section 2 introduces the principle of the corner-smoothing method. In Section 3, two examples are designed to verify the proposed method, and the simulation results are analyzed. The conclusion is given in Section 4.

2. B-Spline Corner Smoothing Method

This section introduces a corner smoothing method using B-spline to generate continuous smooth motion and improve machining efficiency.

2.1. B-Spline Curve

The B-spline curve $C(u)$ is applied to smooth the corner between the linear tool paths, which can be defined as follows [27]:

$$C(u) = \sum_{i=0}^{n} N_{i,p}(u) P_i \; u \in [0,1] \tag{1}$$

where $n+1$ and p represent the number of control points and the order of B-spline, respectively. They are set as 9 and 4, respectively. The knot vector is constructed as [0 0 0 0 0 1/5 2/5 3/5 4/5 1 1 1 1 1]. The basic functions $N_{i,p}(u)$ are given as:

$$\begin{cases} N_{i,0}(u) = \begin{cases} 1 & if \; u_i \le u_{i+1} \\ 0 & else \end{cases} \\ N_{i,p}(u) = \frac{u-u_i}{u_{i+p}-u_i} N_{i,p-1}(u) + \frac{u_{i+p+1}-u}{u_{i+p+1}-u_{i+1}} N_{i+1,p-1}(u) \end{cases} \tag{2}$$

where $0/0 = 0$.

Additionally, the B-spline curve can be simplified as:

$$C(u) = \sum_{i=0}^{8} A_i(u) P_i \; u \in [0,1] \tag{3}$$

where $A_i(u), (i = 0, 1, \ldots, 8)$ is a polynomial, which can be deduced from the basis function $N_{i,p}(u)$. The detailed descriptions $A_i(u)$ are given in Appendix A.

The derivative of B-spline can be expressed as:

$$C(u)' = \frac{dC(u)}{du} = \sum_{i=0}^{8} A_i(u)' P_i \; u \in [0,1] \tag{4}$$

$$C(u)'' = \frac{d^2C(u)}{du^2} = \sum_{i=0}^{8} A_i(u)'' P_i \; u \in [0,1] \tag{5}$$

$$C(u)''' = \frac{d^3C(u)}{du^3} = \sum_{i=0}^{8} A_i(u)''' P_i \; u \in [0,1] \tag{6}$$

In the process of moving along the transition curve $C(u)$, the velocity v, acceleration a and jerk j are typical kinematic parameters, whose vector form can be expressed:

$$\begin{cases} \vec{v} = \frac{dC(u)}{ds}\frac{ds}{dt} = v\vec{T} \\ \vec{a} = \frac{d^2C(u)}{ds^2}\left(\frac{ds}{dt}\right)^2 + \frac{dC(u)}{ds}\frac{d^2s}{dt^2} = kv^2\vec{N} + a\vec{T} \\ \vec{j} = \frac{d^3C(u)}{ds^3}\left(\frac{ds}{dt}\right)^3 + 3\frac{d^2C(u)}{ds^2}\frac{ds}{dt}\frac{d^2s}{dt^2} + \frac{d^3s}{dt^3}\frac{dC(u)}{ds} = \left(\frac{dk}{ds}v^3 + 3avk\right)\vec{N} + \left(j - k^2v^3\right)\vec{T} \end{cases} \tag{7}$$

where

$$v = \frac{ds}{dt}, a = \frac{d^2s}{dt^2}, j = \frac{d^3s}{dt^3}, \vec{T} = \frac{dC(u)}{ds} / \left\| \frac{dC(u)}{ds} \right\|, \vec{N} = \frac{d^2C(u)}{ds^2} / \left\| \frac{d^2C(u)}{ds^2} \right\| \tag{8}$$

$$k = \frac{\|C(u)' \times C(u)''\|}{\|C(u)'\|^3} \tag{9}$$

In Equation (7), t, s and k denote time, arc length and curvature, respectively. As shown in Equation (7), the actual machine motion along the tool path is related to the profiles of the kinematic parameters (i.e., v, a and j) and the continuity of geometric parameters (i.e.,

k and dk/ds). Therefore, in order to enhance the machining efficiency, it is necessary to strengthen the smoothness of the tool path.

For convenience of description, the control point $P_i(i = 0, 1, \ldots, 8)$ of the transition curve in the multi segment linear tool path can be given as $P_{j,i}(j = 0, 1, \ldots, N, i = 0, 1, \ldots, 8)$, N represents the number of corners. In order to obtain the control points, the error feasible area, G^3 continuity and curvature optimization are discussed as follow.

2.1.1. Error Feasible Area

As shown in Figure 1, $\{C_0, \ldots, C_4\}$ represents a linear tool path. The transition allowable error ε denotes the distance between the dotted line and the tool path. The area between two dashed lines is defined as the error feasible area. θ is the angle between the unit vector $\vec{T_1}$ and $\vec{T_2}$. $\vec{T_1} = C_i\vec{C_{i-1}}/\|C_iC_{i-1}\|$, $\vec{T_2} = C_i\vec{C_{i+1}}/\|C_iC_{i+1}\|$, $\vec{T_3} = (\vec{T_1} + \vec{T_2})/\|\vec{T_1} + \vec{T_2}\|$ and $\vec{T_4} = (\vec{T_2} - \vec{T_1})/\|\vec{T_2} - \vec{T_1}\|$. To achieve the allowable error of tool path corner transition, the reconstructed tool path should be within the error feasible area. Depending on the convex hull characteristics and symmetry of B-spline, nine control points of the corner transition curve must be within the error feasible area. Therefore, $P_{j,4}$ is located the angular bisector of θ. $P_{j,3}$ and $P_{j,5}$ are located at the boundary of error feasible area, respectively. $\|P_{j,4}C_j\| = 0.8\varepsilon$ and $\|P_{j,3}P_{j,5}\| = 2l$. l can be expressed as:

$$l = \varepsilon/\cos(\theta/2) + 1.1\varepsilon/\tan(\theta/2) \tag{10}$$

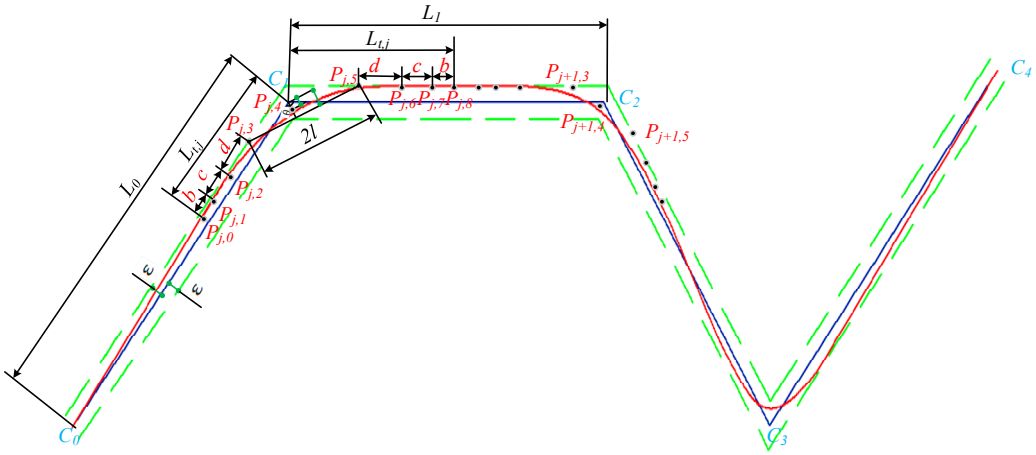

Figure 1. The distribution of corner-smoothing curve.

In order to obtain better corner smoothness, the control points $P_{j,0}$, $P_{j,1}$ and $P_{j,2}$ lie on the linear segment $P_{j,3}P_{j-1,5}$; $P_{j,6}$, $P_{j,7}$ and $P_{j,8}$ lie on the linear segment $P_{j,5}P_{j+1,3}$. Additionally, when $j = 1$, $P_{0,5} \to C_0$. Meanwhile, when $j = N$, $P_{N+1,3} \to C_4$. Thus, the control points of B-spline are calculated as follows:

$$\begin{cases} P_{j,0} = P_{j,1} + b\vec{T_1} \\ P_{j,1} = P_{j,2} + c\vec{T_1} \\ P_{j,2} = P_{j,3} + d\vec{T_1} \\ P_{j,3} = C_j + 1.1\varepsilon\vec{T_3} - l\vec{T_4} \\ P_{j,4} = C_j + 0.8\varepsilon\vec{T_3} \\ P_{j,5} = C_j + 1.1\varepsilon\vec{T_3} + l\vec{T_4} \\ P_{j,6} = P_{j,5} + d\vec{T_2} \\ P_{j,7} = P_{j,6} + c\vec{T_2} \\ P_{j,8} = P_{j,7} + b\vec{T_2} \end{cases} \tag{11}$$

2.1.2. G3 Continuity

In Figure 1, two linear tool paths are connected using the B-spline at junction points $P_{j,0}(u=0)$ and $P_{j,8}(u=1)$. $P_{j,0}$, $P_{j,1}$, $P_{j,2}$, $P_{j,3}$ and $P_{j,5}P_{j,6}$, $P_{j,7}$, $P_{j,8}$ lie on the line segment, respectively. As mentioned above, the B-spline $C(u)$ is 4th order with nine control points to keep G^3 continuity at (0, 1). Since the derivative of the straight line segment is 0 at the connection points, the corresponding derivative of the B-spline should be 0 to obtain G^3 continuous tool path. That is,

$$C''(s)|_{u=0,1} = 0 \tag{12}$$

$$C'''(s)|_{u=0,1} = 0 \tag{13}$$

where

$$C''(s) = C''(u)\big(u'(s)\big)^2 + C'(u)u''(s) \tag{14}$$

$$C'''(s) = C'''(u)\big(u'(s)\big)^3 + 3C''(u)u'(s)u''(s) + C'(u)u'''(s) \tag{15}$$

By mathematic calculation, the sufficient conditions for the establishment of Equations (12) and (13) can be given:

$$C''(u)|_{u=0,1} = 0,\ C'''(u)|_{u=0,1} = 0 \tag{16}$$

$$u''(s)|_{u=0,1} = 0,\ u'''(s)|_{u=0,1} = 0 \tag{17}$$

For corner smoothing B-spline curve, the derivatives of curve parameter u with respect to arc length s can be described as follows.

$$u'(s) = \|C'(u)\|^{-1} \tag{18}$$

$$u''(s) = -C'(u)C''(u)/\|C'(u)\|^4 \tag{19}$$

$$u'''(s) = -\Big\{\Big[(C''(u))^2 + C'(u)C''(u)\Big]\|C'(u)\|^2 - 4\big[C'(u)C'''(u)\big]^2\Big\}/\|C'(u)\|^7 \tag{20}$$

From Equations (18) to (20), it can be seen that the establishment of Equation (16) will lead to the establishment of Equation (17). Substituting Equations (5) and (6) into Equation (16) yields:

$$\begin{cases} C''(u)|_{u=0} = 15(-10c+20b)\vec{T_1} = 0 \\ C'''(u)|_{u=0} = (-(10/3)d+15b-20c)\vec{T_1} = 0 \end{cases} \text{and} \begin{cases} C''(u)|_{u=1} = 15(10c-20b)\vec{T_2} = 0 \\ C'''(u)|_{u=1} = ((10/3)d-15b+20c)\vec{T_2} = 0 \end{cases} \tag{21}$$

Solving Equation (21) obtains,

$$c = 2b,\ d = 3b \tag{22}$$

2.1.3. Corner Transition Length Constraint

As seen in Figure 1, the corners are smoothed by applying B-spline, where $L_{t,j}$ denotes the transition length, which is expressed as:

$$L_{t,1} = \overline{P_{j,3}P_{j,0}} = 6b \tag{23}$$

To avert the overlap of the two corners transition curves, the corners transition length should satisfy the following conditions. That is

$$\begin{cases} L_{t,1} \le \min\big(\overline{P_{1,0}C_0},\ \overline{P_{1,5}P_{2,3}}/2\big) \\ L_{t,j} \le \min\big(\overline{P_{j,3}P_{j-1,5}}/2,\ \overline{P_{j,5}P_{j+1,3}}/2\big)(j=2,\cdots,n-2) \\ L_{t,n-1} \le \min\big(\overline{P_{n-1,3}P_{n-2,5}}/2,\ \overline{P_{n-1,5}C_n}\big) \end{cases} \tag{24}$$

2.2. Curvature Optimization

In the machining process of the corners, the minimum transition velocity $v_{\min-t}$ of corner is the most important factor that limits the machining efficiency, and also affects the acceleration A_n and jerk J_n. According to the literature [28,29], the velocity can be expressed as

$$v_{\min-t} = \min\left(\sqrt{\frac{A_n}{k}}, \sqrt[3]{\frac{J_n}{k^2}}\right) \tag{25}$$

As can be shown in Equation (25), the velocity $v_{\min-t}$ is inversely proportional to the curvature. In order to improve the velocity, smaller curvature should be ensured to obtain higher machining efficiency. In addition, when the curvature reaches the extreme value, it also means that the velocity reaches the extreme value. The increase in the number of curvature extremes leads to the redundant deceleration or acceleration at the corner, which can cause violent fluctuation in speed and the vibration of machining. Therefore, to obtain the unique curvature extremum, the curvature of transitional curve should monotonously increase within [0, 0.5] and monotonically decrease within [0.5, 1]. This constraint relationship can be expressed as:

$$\begin{cases} k_s' = \frac{dk}{du}\frac{du}{ds} \geq 0 & u \in [0, 0.5] \\ k_s' = \frac{dk}{du}\frac{du}{ds} \leq 0 & u \in [0.5, 1] \end{cases} \tag{26}$$

According to the above description, a smoother curve can be obtained by optimizing the curvature to enhance the machining efficiency. Considering the constraints mentioned above, the optimization model can be given:

Objective function:

$$f = \min(k(0.5)) \tag{27}$$

Constraint functions:

$$\begin{cases} L_{t,1} \leq \min\left(\overline{P_{1,0}C_0}, \overline{P_{1,5}P_{2,3}}/2\right) \\ L_{t,j} \leq \min\left(\overline{P_{j,3}P_{j-1,5}}/2, \overline{P_{j,5}P_{j+1,3}}/2\right) (j = 2, \cdots, n-2) \\ L_{t,n-1} \leq \min\left(\overline{P_{n-1,3}P_{n-2,5}}/2, \overline{P_{n-1,5}C_n}\right) \\ k_s' = \frac{dk}{du}\frac{du}{ds} \geq 0 \; u \in [0, 0.5] \\ k_s' = \frac{dk}{du}\frac{du}{ds} \leq 0 \; u \in [0.5, 1] \end{cases} \tag{28}$$

Design variables: b

To solve the above problems, linear programming method is usually used to find the optimal solution. However, these optimal methods would consume much time. Therefore, this paper proposes a simple searching algorithm, which is given as follows.

Step 1: Initialize $b_m = 0, m = 1, \cdots, M$.

Step 2: Determine the control point by Equation (11) and obtain the curve Equation (3) with parameter b.

Step 3: Set $b_m = b_m + \Delta_b$ and $\Delta_b = 0.01$.

Step 4: Calculate the curvature of the transition curve with Equation (27); if Equation (28) is satisfied, the curvature and the corresponding b_m are stored and repeat step 3; if $m = M$, go to step 5.

Step 5: Select b corresponding to the minimum curvature.

2.3. Summary of the Proposed Method

The flowchart of the proposed method can be summarized in Figure 2. Firstly, the error constraint and linear tool path are given. Then, the control points of the B-spline distributing inside and outside the straight line segment of the tool path (i.e., error feasible area) can be calculated with Equation (11). Then, the B-spline $C(u)$ is constructed with Equation (4). To improve the smoothness of transition curve, the optimization model

is established using Equations (27) and (28) and the optimization problem solved using the above linear programming method. Finally, the hybrid tool path with G^3 continuity, including the transition curves and the linear segments, are obtained.

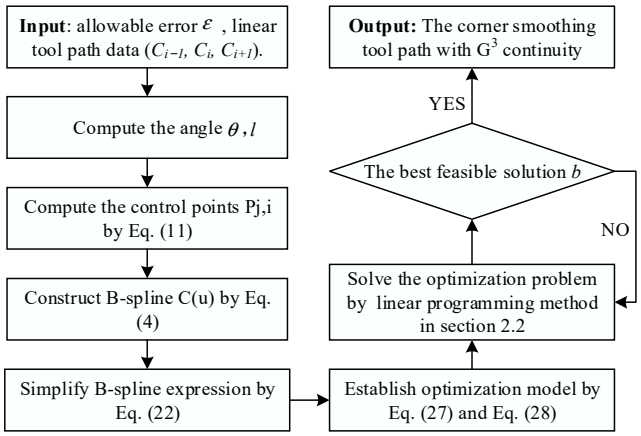

Figure 2. Flowchart of the proposed method.

3. Simulation Experiment Verification

In this section, the proposed algorithm is verified by two examples and compared with Zhao's [11] and Sun's [26] methods. All programs were implemented with MATLAB 2014a on the PC with i7-8700cpu and 16 GB memory.

3.1. Example 1: The 2D Tool Path

As seen in Figure 3, a rhombic tool path is smoothed by the three methods. The curves after transition are drawn with different colors. All methods used the same parameters. Specifically, the transition allowable error ε is 0.05 mm and the maximum velocity is 30 mm/s. The axis velocity, acceleration and jerk limits are 100 mm/s, 1000 mm/s^2 and 120,000 mm/s^3, respectively. From Table 1a, the maximal contour deviation obtained using three methods can satisfy the error constraint. To further compare the feasibility of the proposed method, some criteria (i.e., curvature, curvature derivative, machining time and kinematic fluctuation) were used to evaluate the quality of the smooth tool path.

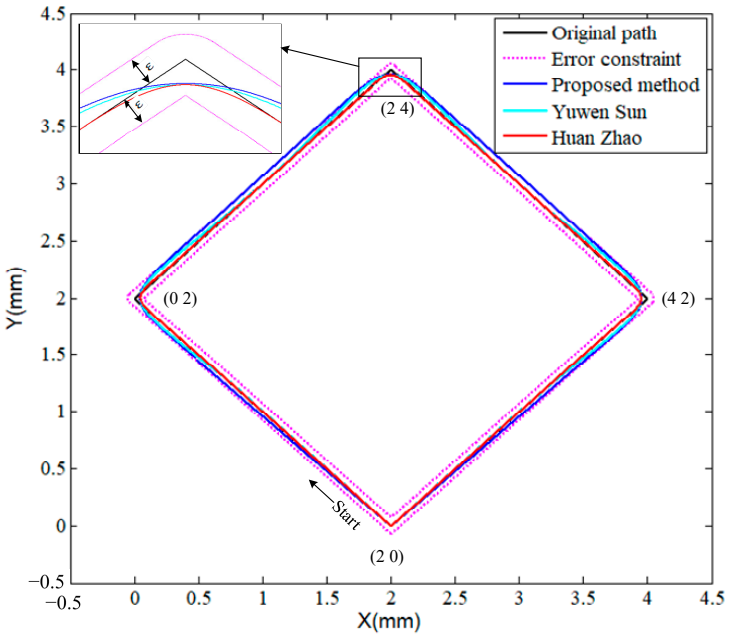

Figure 3. Corner-smoothing using three methods in rhombic tool path.

Table 1. The comparison between three methods.

	Maximal Curvature (mm^{-1})	Maximal Curvature Derivative (mm^{-2})	Machining Time (s)	Maximal Contour Deviation (mm)
(a) The 2D tool path				
Zhao's method	13.3	162.3	0.478	0.05
Sun's method	6.1	43.2	0.457	0.05
Proposed method (base)	5.1	37.5	0.428	0.05
(b) The 3D tool path				
Zhao's method	22.8	446.8	1.58	0.05
Sun's method	9.6	89.4	1.53	0.05
Proposed method (base)	7.0	65.8	1.5	0.05

3.1.1. Curvature and Curvature Derivative

The speed and the machining efficiency can be improved by minimizing the curvature. The curvature and curvature derivative profiles are depicted in Figures 4 and 5, respectively. Table 1a shows the maximal curvature and maximal curvature derivative of the tool paths generated by the three methods. As seen in Figure 4, the profiles of the curvatures obtained by the three methods are continuous, and the proposed method has a lower curvature value than the methods in Zhao's [11] and Sun's [26] works. Especially, in Table 1a, compared with Sun's method and Zhao's method, the maximal curvature extrema is reduced by about 19.6% and 161%, respectively. As shown in Figure 5, the profile of the curvature derivative obtained by Zhao's method is discontinuous at the junction points and middle point of the corner transition curve, which would cause violent machining vibration. The curvature derivative profile of Sun et al. [26] changes frequently, resulting in more fluctuating profiles of the velocity. However, the curvature derivative profile obtained by the proposed method is continuous and the derivative value is also smaller than other methods, which can satisfy the requirements of G^3 continuity and improve the smoothness of corner transition curves. From Table 1a, the G^3 path proposed has lower curvature derivative extrema than the G^2 path generated by the other two methods. The result demonstrates that the proposed method performs better in smoothness, which contributes to obtaining higher machining speed and machining stability.

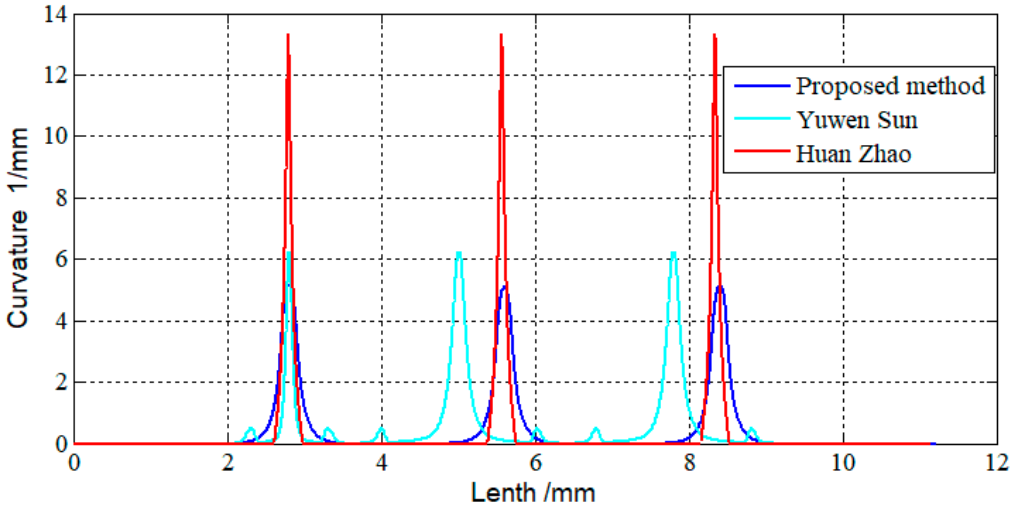

Figure 4. Curvature profiles of 2D tool path.

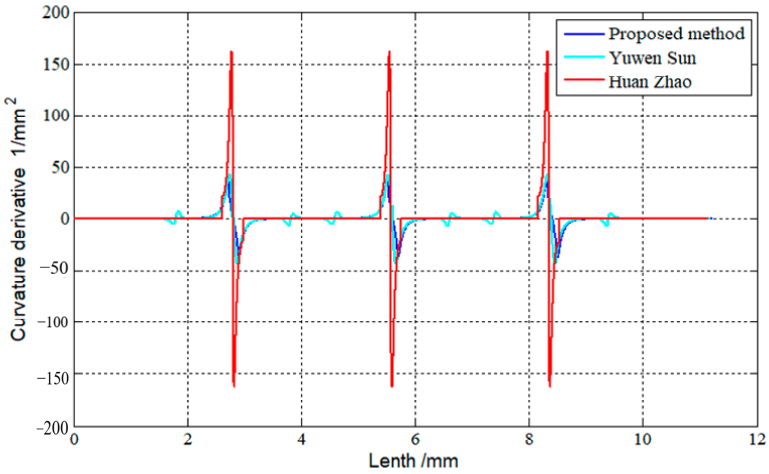

Figure 5. Curvature derivative profiles of 2D tool path.

3.1.2. Machining Time and Kinematic Fluctuation

Machining time is a significant criterion of estimating machining efficiency. Low kinematic fluctuation can decrease machining vibration. As shown in Figure 6, kinematic profiles were calculated using the method developed by Zhao et al. [30]. From Table 1a, it can be seen that the proposed method improves the efficiency since the machining time is 11.7% and 6.8% shorter, respectively. In Figure 6a, the profile of this method also shows that the feedrate along the tool path has little fluctuation and the minimum speed increases significantly, but the fluctuation is obvious with the methods proposed by Zhao et al. [11] and Sun et al. [26]. As can be seen in Figure 6b,c, the acceleration and jerk of the novel corner smoothing method can respect the driving limits. Meanwhile, compared with other methods, the smoothness of acceleration is enhanced by applying the proposed corner smoothing method. Obviously, the example illustrates that the novel smoothing method can enhance the machining efficiency at the corners.

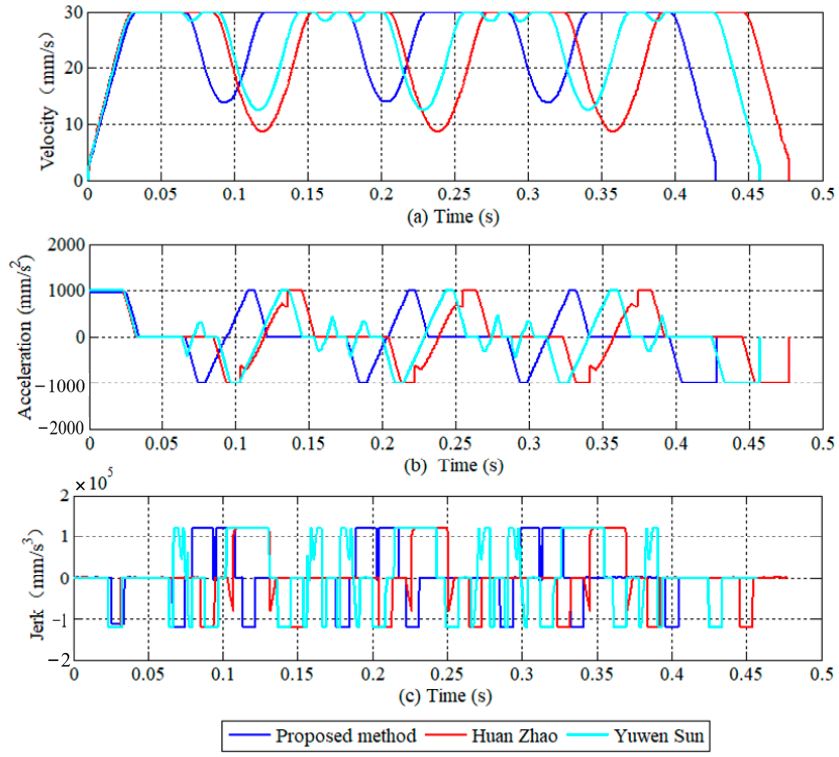

Figure 6. The kinematic profiles (**a**) Velocity profiles. (**b**) Acceleration profiles. (**c**) Jerk profiles.

3.2. Example 2: The 3D Tool Path

To further verify the feasibility of the novel corner smoothing method, a multi segment 3D linear tool path with different transition angles is shown in Figure 7. The parameters are the same as those in example 1. The transition curves obtained by the three methods are also drawn in Figure 7. The curvature and the curvature derivative with respect to the arc length are shown in Figures 8 and 9. As illustrated in the two figures, the smoothing tool path generated by the proposed method has G^3 continuity and there is only one curvature extrema in each transition curve. The curvature value is also smaller than that obtained by the other two methods from Table 1b, which proves the effectiveness of the proposed transition method. In addition, the simulation results show that the smooth performance of the transition curve is good. In addition, the simulation results show that the transition curves have satisfactory smoothness.

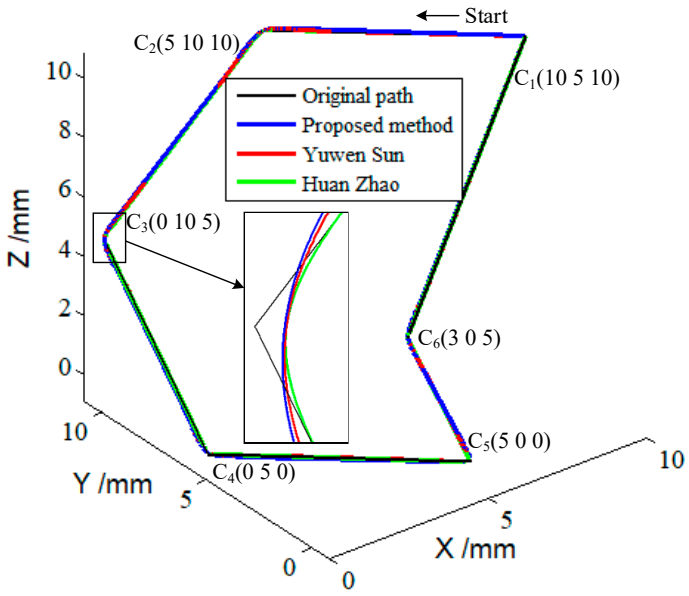

Figure 7. The 3D tool path using three methods.

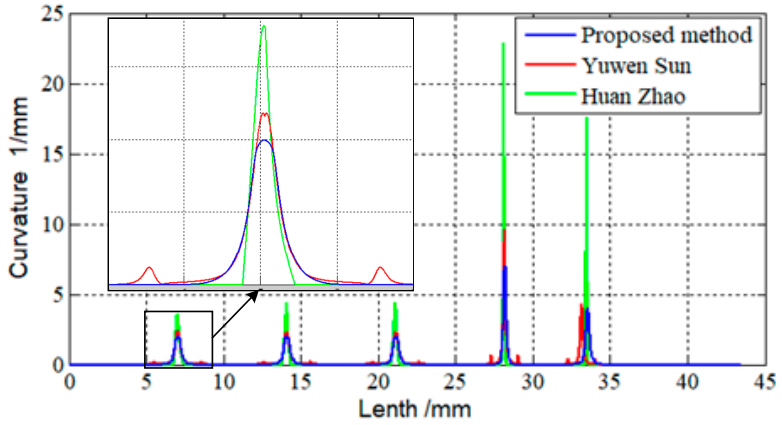

Figure 8. Curvature profiles of 3D tool path.

The profiles of the velocity are shown in Figure 10a. Since the transition curve is smoother, the proposed method can obtain the minimum machining time among the three methods, which can be seen in Table 1b. As observed in Figure 10b–d, the XYZ-axis velocity profiles become smoother. Figures 11a and 12a show the acceleration and jerk profiles generated by the three methods. As shown, the limits of the acceleration and jerk for the drives are fully used and respect the given limits, but the corresponding profiles of the proposed method are smoother and the fluctuation is smaller. Especially in the corner

C_5 and C_6, compared with the frequent acceleration and deceleration processes occurring in the other two methods, the fluctuation in the acceleration and jerk profiles generated by the proposed method is significantly reduced. In addition, it is well-known that the profiles of axial acceleration and jerk would affect the vibration behavior of the machining process [31]. In the Figures 11b–d and 12b–d, the XYZ-axis acceleration and jerk profiles of the proposed method are smoother with less fluctuation, which can reduce the machining vibration. In this case, our optimal method may achieve better contour performance and surface quality.

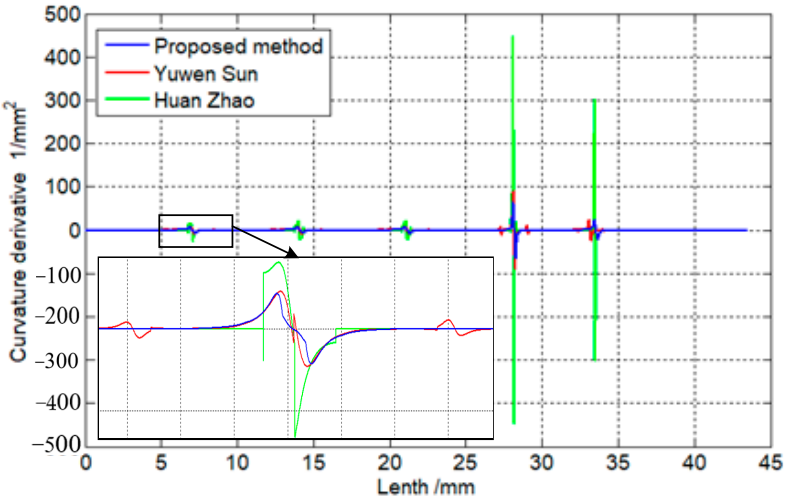

Figure 9. Curvature derivative profiles of 3D tool path.

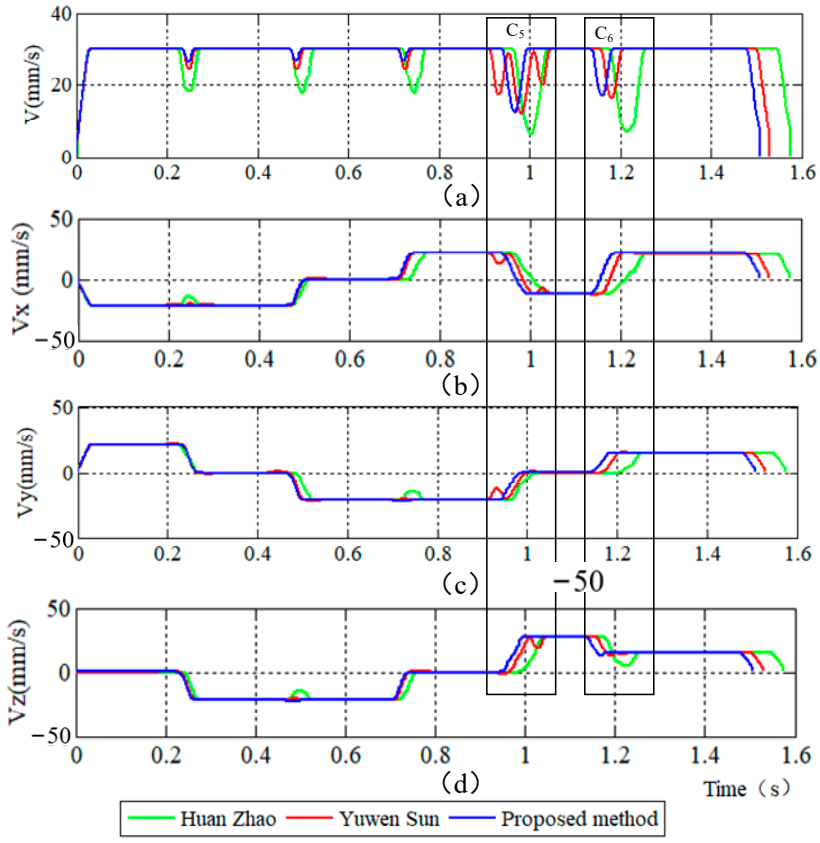

Figure 10. Velocity profiles of 3D tool path.

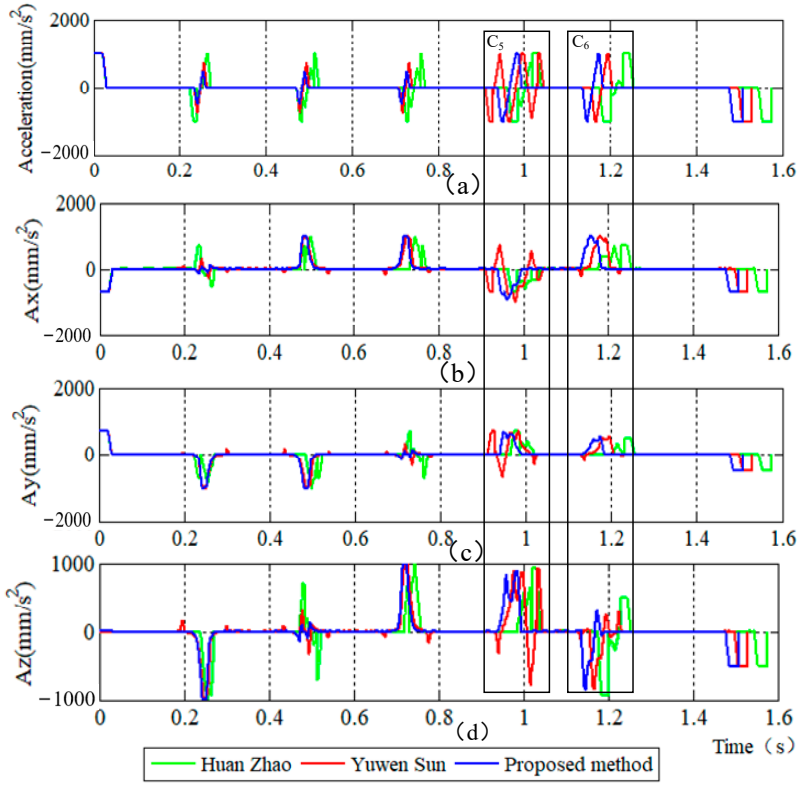

Figure 11. Acceleration profiles of 3D tool path.

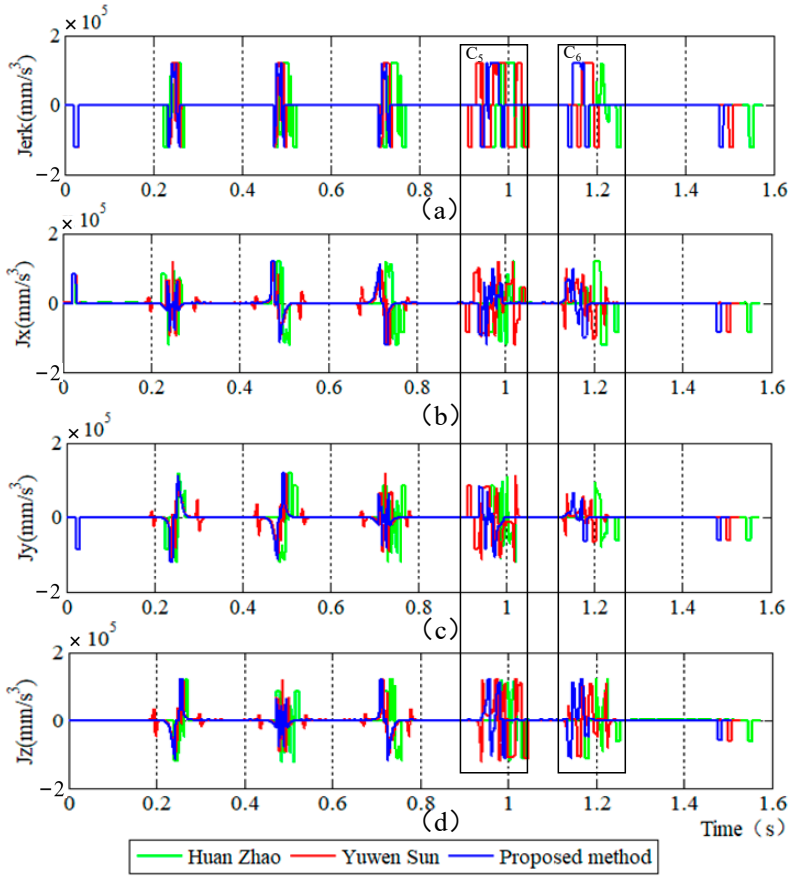

Figure 12. Jerk profiles of 3D tool path.

4. Conclusions

A geometrically smooth tool path plays an important part in realizing high-speed and high-precision NC machining. Thus, a novel corner-smoothing transition method is proposed in this paper. Compared with the previous literatures using higher-order curves with all control points lying in a straight segment and inside of the tool path, the proposed method is based on the error feasible area and reasonably selects the curve control point. Moreover, the curvature of the B-spline transition curves is optimized to enhance the smoothness and keep the G^3 continuity of the mixed tool path, which has smaller curvature and higher feed speed at the sharp corners between the linear tool paths. According to the above advantages, the kinematic profiles of the machining process are relatively smooth with less fluctuation and the machining stability is improved, which can increase machining efficiency and surface quality. Finally, the feasibility and effectiveness of the proposed method were validated by simulations and compared with other already existing methods.

Author Contributions: X.Y. wrote the paper and supervised the work; Y.Y. gave some suggestions on the simulations. All authors have read and agreed to the published version of the manuscript.

Funding: This study was funded partially by the National Science Foundation of China (51775279) and National Key Research and Development Plan of China (2018YFB1309203).

Institutional Review Board Statement: Not applicable.

Informed Consent Statement: Not applicable.

Data Availability Statement: Data sharing is not applicable to this article.

Conflicts of Interest: The authors declare that there is no conflict of interest.

Appendix A

$$A_0 = \begin{cases} 625u^4 - 500u^3 + 150u^2 - 20u + 1 \; u \in [0, 0.2) \\ 0 \; u \in [0.2, 1] \end{cases} \tag{A1}$$

$$A_1 = \begin{cases} -(9375u^4)/8 + 875u^3 - 225u^2 + 20u \; u \in [0, 0.2) \\ (625u^4)/8 - 125u^3 + 75u^2 - 20u + 2 \; u \in [0.2, 0.4) \\ 0 \; u \in [0.4, 1] \end{cases} \tag{A2}$$

$$A_2 = \begin{cases} (53125u^4)/72 - (1375u^3)/3 + 75u^2 \; u \in [0, 0.2) \\ -(14375u^4)/72 + (875u^3)/3 - 150u^2 + 30u - 3/2 \; u \in [0.2, 0.4) \\ (625u^4)/18 - (250u^3)/3 + 75u^2 - 30u + 9/2 \; u \in [0.4, 0.6) \\ 0 \; u \in [0.6, 1] \end{cases} \tag{A3}$$

$$A_3 = \begin{cases} -(15625u^4)/72 + (250u^3)/3 \; u \in [0, 0.2) \\ (14375u^4)/72 - 250u^3 + 100u^2 - (40u)/3 + 2/3 \; u \in [0.2, 0.4) \\ -(8125u^4)/72 + 250u^3 - 200u^2 + (200u)/3 - 22/3 \; u \in [0.4, 0.6) \\ (625u^4)/24 - (250u^3)/3 + 100u^2 - (160u)/3 + 32/3 \; u \in [0.6, 0.8) \\ 0 \; u \in [0.8, 1] \end{cases} \tag{A4}$$

$$A_4 = \begin{cases} (625u^4)/24 \; u \in [0, 0.2) \\ -(625u^4)/6 + (625u^3)/6 - (125u^2)/4 + (25u)/6 - 5/24 \; u \in [0.2, 0.4) \\ (625u^4)/4 - (625u^3)/2 + (875u^2)/4 - (125u)/2 + 155/24 \; u \in [0.4, 0.6) \\ -(625u^4)/6 + (625u^3)/2 - (1375u^2)/4 + (325u)/2 - 655/24 \; u \in [0.6, 0.8) \\ (625u^4)/24 - (625u^3)/6 + (625u^2)/4 - (625u)/6 + 625/24 \; u \in [0.8, 1] \end{cases} \tag{A5}$$

$$A_5 = \begin{cases} 0 \; u \in [0, 0.2) \\ (625u^4)/24 - (125u^3)/6 + (25u^2)/4 - (5u)/6 + 1/24 \; u \in [0.2, 0.4) \\ -(8125u^4)/72 + (3625u^3)/18 - (1525u^2)/12 + (625u)/18 - 253/72 \; u \in [0.4, 0.6) \\ (14375u^4)/72 - (9875u^3)/18 + (6575u^2)/12 - (4235u)/18 + 2663/72 \; u \in [0.6, 0.8) \\ -(15625u^4)/72 + (14125u^3)/18 - (12625u^2)/12 + (11125u)/18 - 9625/72 \; u \in [0.8, 1] \end{cases} \tag{A6}$$

$$A_6 = \begin{cases} 0 \; u \in [0, 0.4) \\ (625u^4)/18 - (500u^3)/9 + (100u^2)/3 - (80u)/9 + 8/9 \; u \in [0.4, 0.6) \\ -(14375u^4)/72 + (9125u^3)/18 - (5675u^2)/12 + (3485u)/18 - 2123/72 \; u \in [0.6, 0.8) \\ (53125u^4)/72 - (44875u^3)/18 + (37525u^2)/12 - (31075u)/18 + 25525/72 \; u \in [0.8, 1] \end{cases} \tag{A7}$$

$$A_7 = \begin{cases} 0 \; u \in [0, 0.6) \\ (625u^4)/8 - (375u^3)/2 + (675u^2)/4 - (135u)/2 + 81/8 \; u \in [0.6, 0.8) \\ -(9375u^4)/8 + (7625u^3)/2 - (18525u^2)/4 + (4985u)/2 - 4015/8 \; u \in [0.8, 1] \end{cases} \tag{A8}$$

$$A_8 = \begin{cases} 0 \; u \in [0, 0.8) \\ 625u^4 - 2000u^3 + 2400u^2 - 1280u + 256 \; u \in [0.8, 1] \end{cases} \tag{A9}$$

References

1. Ferry, W.B.; Altintas, Y. Virtual five-axis flank milling of jet engine impellers part I: Mechanics of five-axis flank milling. *J. Manuf. Sci. Eng.* **2008**, *130*, 11005. [CrossRef]
2. Zhang, Y.; Ye, P.; Zhang, H.; Zhao, M. A Local and Analytical Curvature-Smooth Method with Jerk-Continuous Feedrate Scheduling along Linear Toolpath. *Int. J. Precis. Eng. Manuf.* **2018**, *19*, 1529–1538. [CrossRef]
3. Zhang, Y.; Zhao, M.; Ye, P.; Zhang, H. A G^4 continuous B-spline transition algorithm for cnc machining with jerk-smooth feedrate scheduling along linear segments. *Comput.-Aided Des.* **2019**, *115*, 231–243. [CrossRef]
4. Wu, K.; Krewet, C.; Kuhlenkötter, B. Dynamic performance of industrial robot in corner path with CNC controller. *Robot. Comput.-Integr. Manuf.* **2018**, *54*, 156–161. [CrossRef]
5. Pessoles, X.; Landon, Y.; Rubio, W. Kinematic modelling of a 3-axis NC machine tool in linear and circular interpolation. *Int. J. Adv. Manuf. Technol.* **2010**, *47*, 639–655. [CrossRef]
6. Yang, K.M.; Shi, C.; Ye, P.Q.; Lv, Q. Smooth transfer control algorithm for continuous segment trajectory in computer numerical control systems. *J. Tsinghua Univ. (Sci. Technol.)* **2007**, *47*, 1295–1299.
7. Bi, Q.; Wang, Y.; Zhu, L.; Ding, H. A practical continuous curvature Bezier transition algorithm for high-speed machining of linear tool path. In *Intelligent Robotics and Applications, Proceedings of the 4th International Conference, (ICIRA 2011), Aachen, Germany, 6–8 December 2011*; Jeschke, S., Liu, H., Schilberg, D., Eds.; Springer: Berlin/Heidelberg, Germany, 2011; pp. 465–476.
8. Xu, D.; Jie, H.; Li-Min, Z. A locally optimal transition method with analytical calculation of transition length for computer numerical control machining of short line segments. *Proc. Inst. Mech. Eng.* **2018**, *232*, 2409–2419.
9. Pateloup, V.; Duc, E.; Ray, P. B-spline approximation of circle arc and straight line for pocket machining. *Comput.-Aided Des.* **2010**, *42*, 817–827. [CrossRef]
10. Zhang, L.B.; You, Y.P.; He, J.; Yang, X.F. The transition algorithm based on parametric spline curve for high-speed machining of continuous short line segments. *Int. J. Adv. Manuf. Technol.* **2011**, *52*, 245–254. [CrossRef]
11. Zhao, H.; Zhu, L.M.; Ding, H. A real-time look-ahead interpolation methodology with curvature-continuous b-spline transition scheme for cnc machining of short line segments. *Int. J. Mach. Tools Manuf.* **2013**, *65*, 88–98. [CrossRef]
12. Han, J.; Jiang, Y.; Tian, X.; Chen, F.; Lu, C.; Xia, L. A local smoothing interpolation method for short line segments to realize continuous motion of tool axis acceleration. *Int. J. Adv. Manuf. Technol.* **2018**, *95*, 1729–1742. [CrossRef]
13. Sencer, B.; Ishizaki, K.; Shamoto, E. A curvature optimal sharp corner smoothing algorithm for high-speed feed motion generation of NC systems along linear tool paths. *Int. J. Adv. Manuf. Technol.* **2015**, *76*, 1977–1992. [CrossRef]
14. Farouki, R.T. Construction of G2 rounded corners with Pythagorean-hodograph curves. *Comput. Aided Geom. Des.* **2014**, *31*, 127–139. [CrossRef]
15. Shi, J.; Bi, Q.Z.; Wang, Y.H.; Liu, G. Development of real-time look-ahead methodology based on quintic PH curve with G^2 continuity for high-speed machining. *Appl. Mech. Mater.* **2014**, *464*, 258–264. [CrossRef]
16. Huang, X.; Zhao, F.; Tao, T.; Mei, X. A newly developed corner smoothing methodology based on clothoid splines for high speed machine tools. *Robot. Comput.-Integr. Manuf.* **2021**, *70*, 102106. [CrossRef]
17. Fan, W.; Lee, C.H.; Chen, J.H. A realtime curvature-smooth interpolation scheme and motion planning for CNC machining of short line segments. *Int. J. Mach. Tools Manuf.* **2015**, *96*, 27–46. [CrossRef]

18. Yang, X.; You, Y.; Yang, W.A. Simultaneous optimization of curvature and curvature variation for tool path generation in high-speed milling of corners. *J. Braz. Soc. Mech. Sci. Eng.* **2022**, *44*, 68. [CrossRef]
19. Tulsyan, S.; Altintas, Y. Local toolpath smoothing for five-axis machine tools. *Int. J. Mach. Tools Manuf.* **2015**, *96*, 15–26. [CrossRef]
20. Zhang, Y.; Mingyong, Z.; Peiqing, Y.; Jiang, J.; Zhang, H. Optimal curvature-smooth transition and efficient feedrate optimization method with axis kinematic limitations for linear toolpath. *Int. J. Adv. Manuf. Technol.* **2018**, *99*, 169–179. [CrossRef]
21. Du, X.; Wang, B. A C^3-continuous NURBS transition scheme for the CNC machining of short linear segments. *Precis. Eng.* **2022**, *73*, 1–10. [CrossRef]
22. Hu, Q.; Chen, Y.; Yang, J.; Zhang, D. An analytical C^3 continuous local corner smoothing algorithm for four-axis computer numerical control machine tools. *J. Manuf. Sci. Eng.* **2018**, *140*, 051004. [CrossRef]
23. Hu, Q.; Chen, Y.; Jin, X.; Yang, J. A real-time C^3 continuous tool path smoothing and interpolation algorithm for five-axis machine tools. *J. Manuf. Sci. Eng.* **2020**, *142*, 041002. [CrossRef]
24. Sun, S.; Altintas, Y. A G^3 continuous tool path smoothing method for 5-axis CNC machining. *CIRP J. Manuf. Sci. Technol.* **2021**, *32*, 529–549. [CrossRef]
25. Sun, S. A G^3 continuous five-axis tool path corner smoothing method with improved machining efficiency and accurately controlled deviation of tool axis orientation. *Int. J. Adv. Manuf. Technol.* **2022**, *119*, 7003–7024. [CrossRef]
26. Xu, F.; Sun, Y. A circumscribed corner rounding method based on double cubic B-splines for a five-axis linear tool path. *Int. J. Adv. Manuf. Technol.* **2018**, *94*, 451–462. [CrossRef]
27. Moore, P.; Molloy, D. Efficient Energy Evaluations for Active B-Spline/NURBS Surfaces. *Comput.-Aided Des.* **2014**, *47*, 12–31. [CrossRef]
28. Lee, A.C.; Lin, M.T.; Pan, Y.R.; Lin, W.Y. The feedrate scheduling of nurbs interpolator for CNC machine tools. *Comput.-Aided Des.* **2011**, *43*, 612–628. [CrossRef]
29. Lai, J.Y.; Lin, K.Y.; Tseng, S.J.; Ueng, W.D. On the development of a parametric interpolator with confined chord error, feedrate, acceleration and jerk. *Int. J. Adv. Manuf. Technol.* **2008**, *37*, 104–121. [CrossRef]
30. Zhao, X.; Zhao, H.; Yang, J.; Ding, H. An adaptive feedrate scheduling method with multi-constraints for five-axis machine tools. In Proceedings of the International Conference on Intelligent Robotics and Applications 2015, Portsmouth, UK, 24 August 2015; Springer: Cham, Switzerland, 2015; pp. 553–564.
31. Barre, P.; Bearee, R.; Borne, P.; Dumetz, E. Influence of a jerk controlled movement law on the vibratory behaviour of highdynamics systems. *J. Intell. Robot. Syst.* **2005**, *42*, 275–293. [CrossRef]